

# Crystal Structure and Ionic Conduction Mechanism of AgHgSX (X = Br, I)

Masakazu Moro'oka,\* Hiroshi Ohki, Koji Yamada, and Tsutomu Okuda

Department of Chemistry, Graduate School of Science, Hiroshima University,  
1-3-1 Kagamiyama, Higashihiroshima, Hiroshima 739-8526

Received October 16, 2003; E-mail: morooka@hiroshima-u.ac.jp

New Ag<sup>+</sup> ionic conductors AgHgSX (X = Br, I) were synthesized by solid-state reactions of AgX (X = Br, I) and HgS. AgHgSI shows a phase transition at 578 K. The crystal structure of the high temperature phase has been determined to be  $P2_12_12_1$  (No. 19) by the Rietveld refinement using the powder X-ray diffraction pattern. The electric conductivity at 500 K measured by the AC impedance method was  $2.6 \times 10^{-4} \text{ S cm}^{-1}$  for the high temperature phase of AgHgSI,  $1.2 \times 10^{-4} \text{ S cm}^{-1}$  for the low temperature phase of AgHgSI, and  $1.1 \times 10^{-4} \text{ S cm}^{-1}$  for AgHgSBr. The charge density analysis of the AgHgSX (X = Br, I) clearly showed the Ag<sup>+</sup> ionic conduction path when analyzed by the Maximum Entropy Method (MEM) combined with Rietveld analysis.

It is well known that silver halides are cationic conductors. Many double salts of these halides with other compounds show higher conductivity at low temperature. RbAg<sub>4</sub>I<sub>5</sub> is good examples of a superionic conductor at room temperature discovered by the synthesis of double salts.<sup>1</sup>

The family of MHgSX (M = Cu, Ag; X = Cl, Br, I) has been prepared by combining copper or silver halides with HgS. The crystal structures of this material group have been examined by several authors: Gullio et al.<sup>2</sup> and Beck et al.<sup>3</sup> independently determined the crystal structures of CuHgSCl and CuHgSBr at room temperature; the structures were different from each other. Beck et al. also reported the crystal structures of CuHgSeBr, AgHgSBr, and AgHgSI.<sup>4</sup> AgHgSCl was synthesized and examined by Blachnik et al.<sup>5</sup> They reported the phase diagram of the AgCl–HgS system and the lattice parameters of the constituent substances.

In this work, we investigated phase transition, crystal structures, and electric conductivities of AgHgSX (X = Br, I). The crystal structure of new phase for AgHgSI was determined by a Rietveld analysis of powder X-ray diffraction patterns. The electric conductivities of these materials were measured by an AC impedance method, whereas the major charge carrier was determined by use of transport number measurements. The electric conduction mechanisms of AgHgSX (X = Br, I) will be discussed using the results obtained from a Maximum Entropy Method (MEM) combined with the Rietveld analysis.

## Experimental

AgHgSI was prepared by heating a stoichiometric mixture of AgI (Kanto Chemical Co. Inc., purity 99.0%) and red-HgS (Kojundo Chemical Lab. Co., purity 99.9%) in an evacuated Pyrex tube at ca. 473 K for 1 week. AgHgSBr was synthesized from AgBr (Soekawa Chemical Co. Ltd., purity 99.0%) and red-HgS at ca. 573 K for 1 week.

Differential thermal analysis (DTA) measurements were carried out between 100 K and 650 K by use of a homemade

apparatus.

Powder X-ray diffraction patterns were measured on a Rigaku RINT-2000 system using Cu K $\alpha$  radiation with a scan rate of 0.5 degree/min and a scan step of 0.02 degree.

The crystal structure of AgHgSI was initially guessed by the program EXPO,<sup>6</sup> and successively refined by the Rietveld method using RIETAN-2000 program.<sup>7</sup>

The electron density of the crystal was analyzed by means of the Maximum Entropy Method (MEM) combined with the pattern fitting.<sup>8</sup> During the electron density analyses, the unit cells of the crystals were divided into edges of ca. 0.1 Å each.

The electric conductivities were determined by an AC impedance method. The complex impedance measurements were performed by the two-terminal method using a computer interfaced HIOKI 3532 LCR meter (42 Hz–5 MHz) in the temperature range from 300 to 500 K. The pellet sizes were 13 mm in diameter and 1.0–1.4 mm in thickness. Carbon paint was applied on both sides of the pellet and electrodes to insure good electric contact with each other. The temperature of the sample was controlled within  $\pm 1$  K using a Chino KP1000 temperature controller equipped with Cu–Constantan thermocouples.

The ionic transport measurements were carried out using an “ion blocking” method and a non-“ion blocking” method. (i) In the non-“ion blocking” method, two pellets of the sample were sandwiched between copper electrodes. A constant DC current of 0.09 mA was applied across the sample for 3 days at 400 K using an ADVANTEST programmable DC voltage/current generator (TR6142). (ii) In the “ion blocking” method, two pellets of the sample were sandwiched between copper electrodes with carbon paint on both sides of the pellets. A constant DC voltage of 1 V was applied across the sample for 1–2 days at room temperature by use of the ADVANTEST generator (TR6142). This method induces a polarization effect across the sample, if the substance has ionic conductivity. The ionic transport number ( $t_{\text{ion}}$ ) of the sample was estimated using the relation  $t_{\text{ion}} = I_{\text{ion}}/I_{\text{tot}}$ , where  $I_{\text{ion}}$  is the current due to the mobile ions and  $I_{\text{tot}}$  is the total current due to all charge carriers.

### Results

**DTA.** Figure 1 shows the observed DTA curves of  $\text{AgHgSI}$ . An endothermic peak appeared at 578 K on heating, but no exothermic peak was found on cooling in the first run. No thermal anomaly was observed in the second run up to 593 K, where the sample decomposition occurred. Hereafter, these two phases of  $\text{AgHgSI}$  are designated as  $\alpha$  and  $\beta$  forms, from the high temperature side. Both phases are stable at room temperature toward air and moisture.  $\beta$ - $\text{AgHgSI}$  could not be obtained by annealing  $\alpha$ - $\text{AgHgSI}$  at 473 K for 1 week.

$\text{AgHgSBr}$  showed no thermal anomaly and decomposed at 613 K (not shown here).

**Crystal Structure of  $\beta$ - $\text{AgHgSI}$  and  $\text{AgHgSBr}$ .** It was found that the crystal structure reported by Beck et al. corresponds to the  $\beta$ - $\text{AgHgSI}$  according to the powder X-ray diffrac-

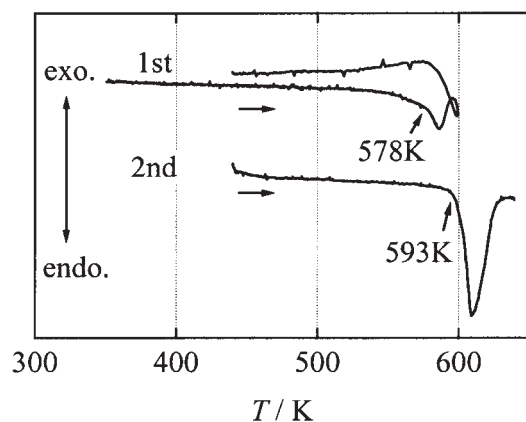


Fig. 1. DTA curves of  $\text{AgHgSI}$ .

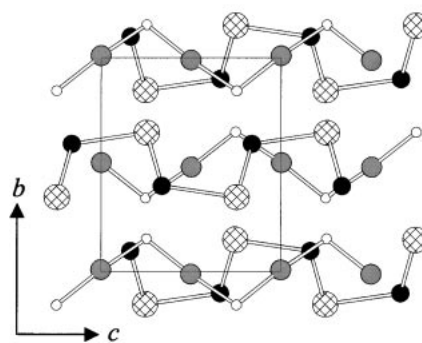
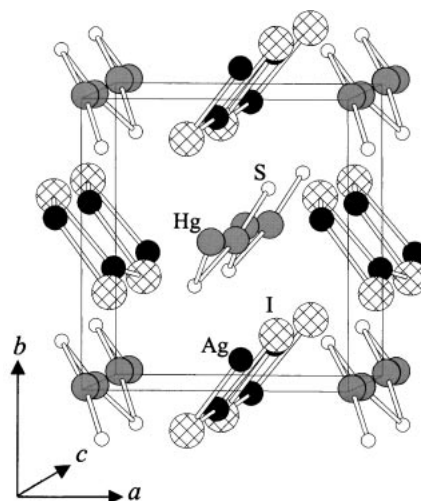


Fig. 3. Crystal structure of  $\alpha$ - $\text{AgHgSI}$  at room temperature.

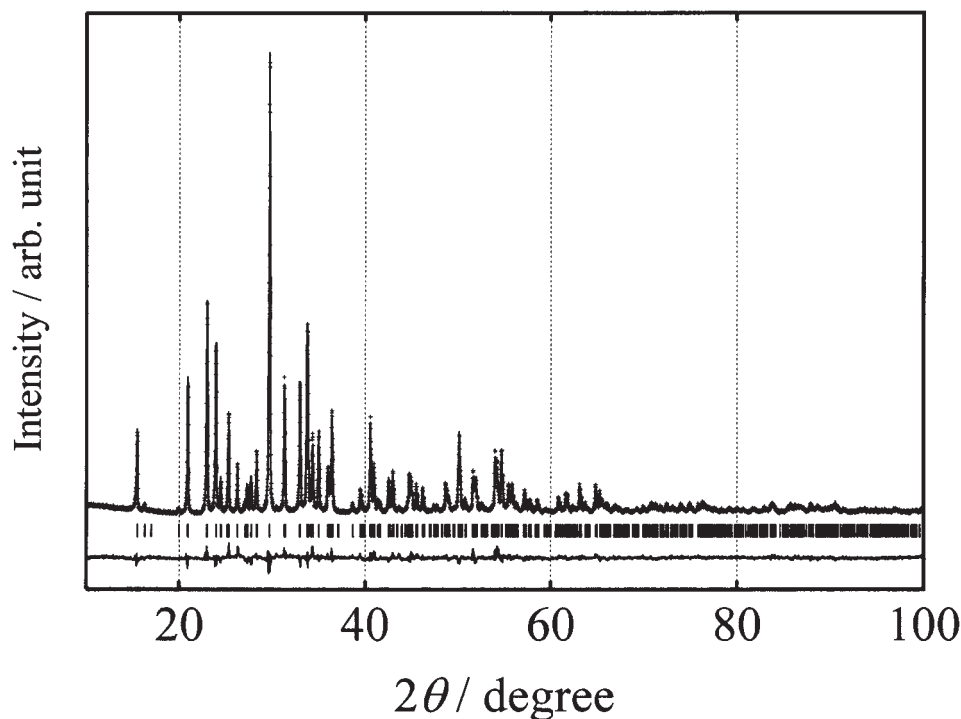


Fig. 2. Observed (cross) and calculated (solid line) X-ray diffraction pattern of  $\alpha$ - $\text{AgHgSI}$  at room temperature. Tick marks indicate the positions of allowed Bragg reflections. The difference line, observed minus calculated, is located at the bottom of the figure.

Table 1. Experimental Conditions and Crystallographic Data of  $\alpha$ -AgHgSI

Compound	$\alpha$ -AgHgSI
Space group	$P2_12_12_1$ (No. 19)
Crystal system	Orthorhombic
Lattice constants/ $\text{\AA}$	$a = 7.7275(2)$ $b = 8.4695(2)$ $c = 7.0710(2)$
Volume/ $\text{\AA}^3$	462.79(2)
Range $2\theta/^\circ$	10–100
$Z$	4
Scan step/ $^\circ$	0.02
Structural parameters	16
Profile parameters	10 + 15 <sup>a)</sup>
Number of reflections	291
$R_p/\%$	6.28
$R_{wp}/\%$	8.19
$R_{exp}/\%$	4.95
$R_{Bragg}/\%$	3.51

a) Partial profile relaxation [7].

Table 2. Atomic Positions and Isotropic Parameters of  $\alpha$ -AgHgSI

Atom	$x$	$y$	$z$	$U_{iso}/\text{\AA}^2$
Ag	0.1729(4)	0.4015(4)	0.0877(4)	0.0808(16)
Hg	0.2640(3)	−0.0105(2)	0.2491(3)	0.0365(6)
S	0.3571(1)	0.1543(9)	1.0029(18)	0.0148(24)
I	0.1137(3)	0.3494(2)	0.5039(4)	0.0208(7)

Table 3. Interatomic Distances ( $\text{\AA}$ ) and Bond Angles ( $^\circ$ ) of  $\alpha$ -AgHgSI

Ag <sup>i</sup> –I <sup>i</sup>	3.011(4)	I–Ag–I	114.55(12)
Ag <sup>i</sup> –I <sup>ii</sup>	2.743(3)	Ag–I–Ag	90.39(11)
Hg <sup>i</sup> –S <sup>i</sup>	2.344(10)	S–Hg–S	173.1(2)
Hg <sup>i</sup> –S <sup>ii</sup>	2.362(10)	Hg–S–Hg	98.8(2)

(i)  $x, y, z$ . (ii)  $\bar{x} + 1/2, \bar{y}, z + 1/2$ .

tion pattern. AgHgSBr was identical with the one reported by Beck et al., as is also confirmed by the powder X-ray diffraction pattern.

**Rietveld Analysis for  $\alpha$ -AgHgSI.** The XRD pattern of the  $\alpha$ -AgHgSI could be indexed in the orthorhombic system,  $P2_12_12_1$ . Figure 2 shows the result of the Rietveld refinement using powder X-ray diffraction pattern of  $\alpha$ -AgHgSI at room temperature. Figure 3 depicts the crystal structure of  $\alpha$ -AgHgSI determined by the Rietveld analysis. Table 1 summarizes the experimental conditions and crystallographic data. Table 2 shows the atomic positions and isotropic thermal parameters. Table 3 lists selected interatomic distances and bond angles.

**MEM Analysis.** The electron density maps along (100) plane for  $\alpha$ -AgHgSI at room temperature are drawn in Fig. 4. Figure 5 shows the charge density maps along the same plane as in Fig. 4, but at 400 K. Figures 6 and 7 depict the electron density maps along (010) plane for  $\beta$ -AgHgSI at room temperature and 400 K, respectively. Figures 8 and 9 illustrate the electron density maps along (010) plane for AgHgSBr at room

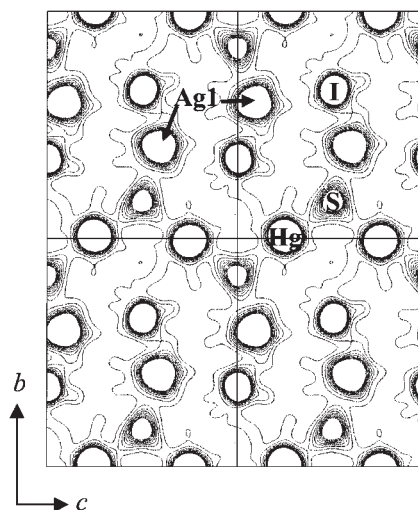


Fig. 4. The charge density map at room temperature determined by MEM for  $\alpha$ -AgHgSI. This figure is projected onto (100) plane between  $x = 0$  and  $x = 0.5$ . The contour lines are drawn from 0.0 to 100.0  $\text{e \AA}^{-3}$  at 5.0  $\text{e \AA}^{-3}$  intervals. The map contains four unit cells.

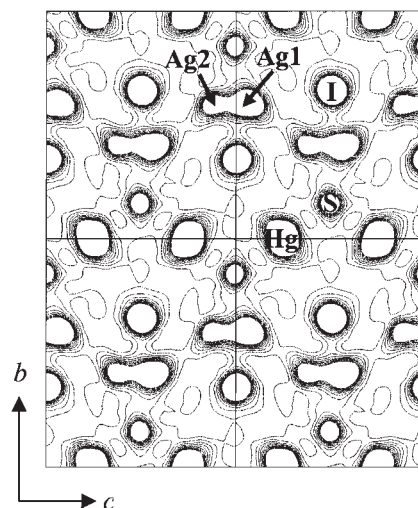


Fig. 5. The charge density map at 400 K determined by MEM for  $\alpha$ -AgHgSI. This figure is projected onto (100) plane between  $x = 0$  and  $x = 0.5$ . The contour lines are drawn from 0.0 to 100.0  $\text{e \AA}^{-3}$  at 5.0  $\text{e \AA}^{-3}$  intervals. The map contains four unit cells.

temperature and 500 K, respectively. All figures were drawn by VENUS system developed by Dilanian and Izumi.

**Conductivity.** Figure 10 represents the electric conductivities plotted against the inverse temperature for AgHgSX. With increasing temperature, the conductivity of each sample increased monotonously. The electric conductivities at 500 K measured by the AC impedance method were  $2.6 \times 10^{-4} \text{ S cm}^{-1}$  for  $\alpha$ -AgHgSI,  $1.2 \times 10^{-4} \text{ S cm}^{-1}$  for  $\beta$ -AgHgSI, and  $1.1 \times 10^{-4} \text{ S cm}^{-1}$  for AgHgSBr. The electric conductivity increased in the order of  $\text{AgHgSBr} < \beta\text{-AgHgSI} < \alpha\text{-AgHgSI}$ .

**Ionic Transport.** In the measurements by non-“ion blocking” method, the silver metallic luster was separated out between the sample and negative electrode. The ionic transport

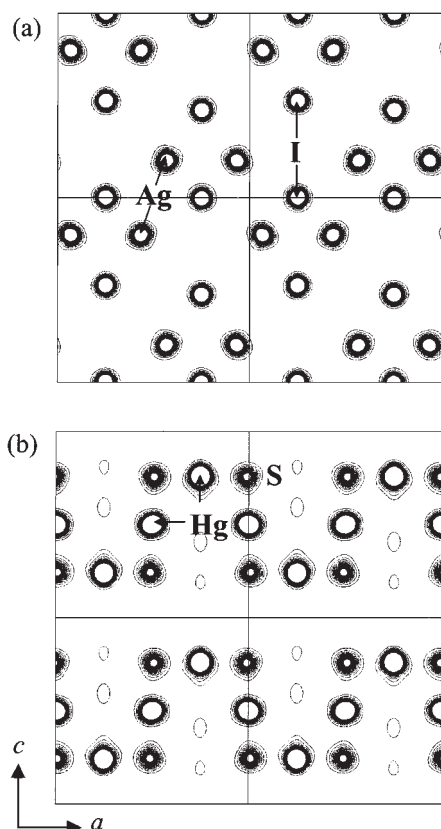


Fig. 6. The charge density maps at room temperature determined by MEM along (010) plane for  $\beta$ -AgHgSI (a) at Ag–I chain ( $y = 1/2$ ) and (b) at Hg–S chain ( $y = 0$ ). The contour lines are drawn from 0.0 to 100.0  $\text{e} \text{Å}^{-3}$  at 5.0  $\text{e} \text{Å}^{-3}$  intervals, respectively. Both maps contain four unit cells.

number values determined by “ion blocking” method revealed that the ionic contribution to the all conduction process is 93% for  $\alpha$ -AgHgSI, 95% for  $\beta$ -AgHgSI, and 98% for AgHgSBr.

### Discussion

#### Phase Transition and Crystal Structure of $\alpha$ -AgHgSI.

The phase transition from  $\beta$ -AgHgSI to  $\alpha$ -AgHgSI arises at 578 K on heating.  $\alpha$ -AgHgSI constitutes the metastable phase at room temperature, because the reversible modification does not rapidly appear on cooling. In addition,  $\alpha$ -AgHgSI is single phase, since the decompose point was at 593 K.

$\alpha$ -AgHgSI was obtained by heating  $\beta$ -AgHgSI at 585 K for 1 hour. The powder X-ray pattern of the constant diffraction intensity includes no starting materials and no impurity. All peaks were conclusively indexed as space group  $P2_12_12_1$  and  $R_p$  factor dropped to 6.28% shown in Table 1. Then, appropriate atomic positions and isotropic parameters were determined as shown in Table 2. The crystal structure was very similar to that of the analogous compound CuHgSI.<sup>9</sup> As shown in Fig. 3, Ag–I and Hg–S bonds form zig-zag chains along the crystallographic  $c$ -axis. These chains arrange alternatively along the  $a$ - and  $b$ -axes. Cations are tetrahedrally coordinated by anions. All atoms occupy their sites completely at room temperature, but the isotropic parameter  $U_{\text{iso}}$  of Ag atom is larger than those of the other sites. This implies that  $\alpha$ -AgHgSI tends to be  $\text{Ag}^+$  ion conductors.

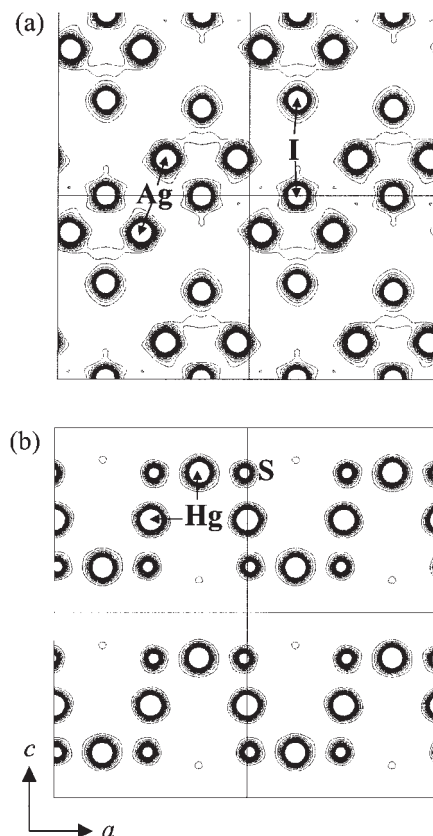


Fig. 7. The charge density maps at 400 K determined by MEM along (010) plane for  $\beta$ -AgHgSI (a) at Ag–I chain ( $y = 1/2$ ) and (b) at Hg–S chain ( $y = 0$ ). The contour lines are drawn from 0.0 to 100.0  $\text{e} \text{Å}^{-3}$  at 5.0  $\text{e} \text{Å}^{-3}$  intervals, respectively. Both maps contain four unit cells.

**Crystal Structures of  $\beta$ -AgHgSI and AgHgSBr.** The crystal structures for  $\beta$ -AgHgSI and AgHgSBr have been determined by Beck et al.<sup>4</sup> The high temperature phases of CuHgSBr and CuHgSBr have analogous structures.<sup>3,10</sup> In these structures, as shown in Fig. 11, S–Hg–S is linked alternatively by Hg atoms; Ag and halogens form distorted squares. Hg atoms are surrounded by two sulfurs and four halogens, whereas Ag ions are tetrahedrally coordinated by two sulfurs and two halogens.

As was mentioned in the previous section, the forms of Hg–S chains in the  $\alpha$ -AgHgSI are different from that in the  $\beta$ -AgHgSI. However, the bond lengths and bond angles are not so different, and this may be the reason why the  $\alpha$ -AgHgSI is very stable.

**Transport Number Measurements.** As shown previously, the values of ionic transport number determined by means of the “ion blocking” method shows that  $\text{Ag}^+$  ions constitute the major charge carriers in all samples. This fact clearly implies that the electronic contribution to the conduction process in these substances is less than 10%.

**Conduction Mechanism.** As shown in Fig. 10, the  $\text{Ag}^+$  ion conductivity for  $\alpha$ -AgHgSI was highest among those of the studied samples. The activation enthalpy  $\Delta H$  is obtained from the following equation:<sup>11</sup>

$$\sigma(T) = \sigma_0 \exp(-\Delta H/RT), \quad (1)$$

where  $\sigma$  is the electric conductivity. By fitting Eq. 1 to the ob-



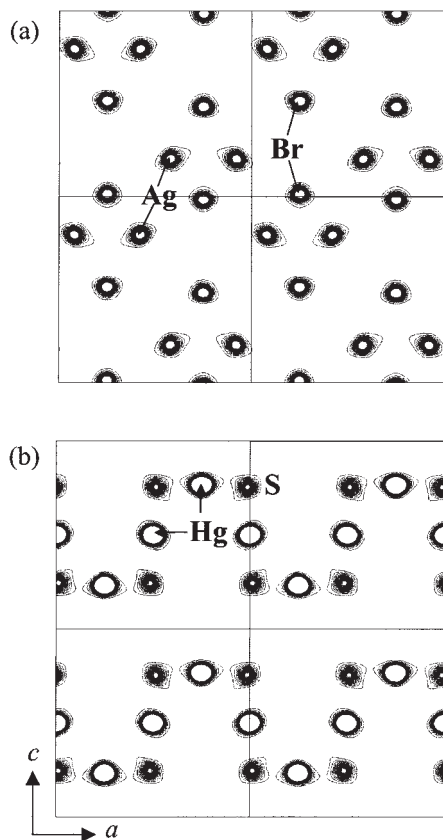


Fig. 8. The charge density maps at room temperature determined by MEM along (010) plane for AgHgSBr (a) at Ag–Br chain ( $y = 1/2$ ) and (b) at Hg–S chain ( $y = 0$ ). The contour lines are drawn from 0.0 to 100.0  $\text{e} \text{Å}^{-3}$  at 5.0  $\text{e} \text{Å}^{-3}$  intervals, respectively. Both maps contain four unit cells.

served data, the activation enthalpies were evaluated to be 36  $\text{kJ mol}^{-1}$  for  $\alpha$ -AgHgSI, 42  $\text{kJ mol}^{-1}$  for  $\beta$ -AgHgSI, and 53  $\text{kJ mol}^{-1}$  for AgHgSBr. The difference of the activation enthalpies will be discussed below in detail.

**$\alpha$ -AgHgSI:** The particular conduction path of  $\alpha$ -AgHgSI could be found by MEM analysis. Figures 4 and 5 illustrate the electron density maps along the (100) plane at room temperature and 400 K, respectively. At room temperature, Ag and I atoms localize in each site. The electron density distribution of Ag atom, however, was clearly prolonged along the  $c$ -axis at 400 K, but that of I atom shows almost same shape. Then, no difference in electron density distributions was seen in Hg–S chains at room temperature and at 400 K. This fact strongly indicates that each  $\text{Ag}^+$  ion moves a certain direction at 400 K. It seems that Ag ions occupy two sites, which will be called Ag1 and Ag2. Moreover, the electron density of Ag2 site spreads over the Ag1 site. The Ag1 site coordinated by 4 anions consisting of S and I corresponds to the Ag position in the crystal structure at room temperature. The Ag2 site is the novel location emerging with elevated temperature; Ag1 and Ag2 sites possess the similar chemical environment. Thus, the electron density of Ag2 will derive from that of Ag1. In fact, the isolation is supported by the facts that these site occupancies at 400 K could be determined as 70% for Ag1 site and 30% for Ag2 site by the Rietveld analysis. At the same temperature, each iso-

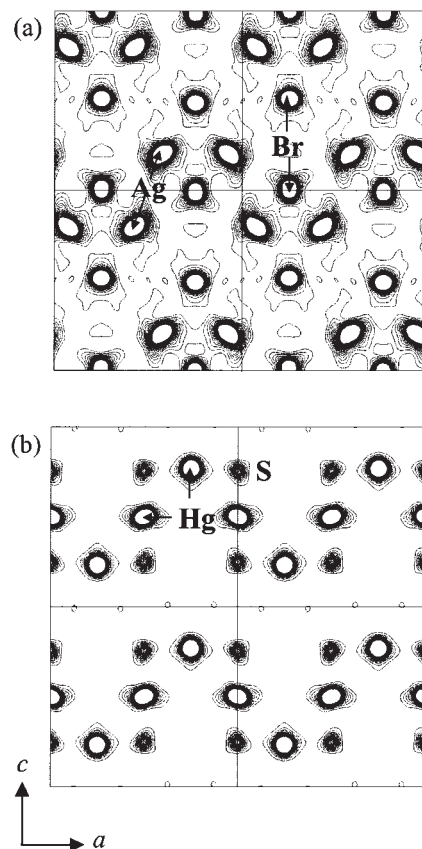


Fig. 9. The charge density maps at 500 K determined by MEM along (010) plane for AgHgSBr (a) at Ag–Br chain ( $y = 1/2$ ) and (b) at Hg–S chain ( $y = 0$ ). The contour lines are drawn from 0.0 to 100.0  $\text{e} \text{Å}^{-3}$  at 5.0  $\text{e} \text{Å}^{-3}$  intervals, respectively. Both maps contain four unit cells.

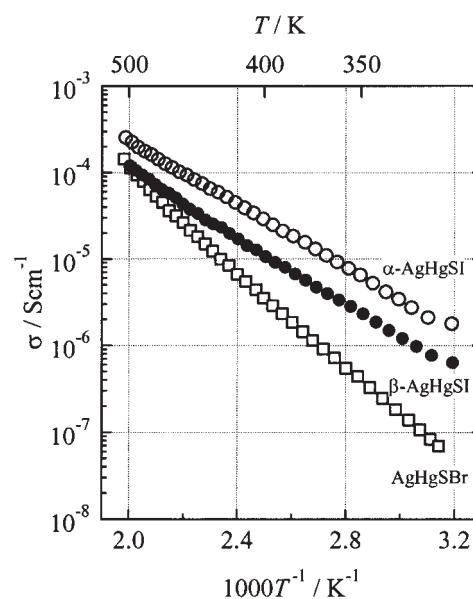


Fig. 10. Temperature dependence of electric conductivities in AgHgSX ( $X = \text{Br}, \text{I}$ ).

tropic parameter  $U_{\text{iso}}$  was 0.075(5) and 0.017(9)  $\text{Å}^2$  for Ag1 and Ag2 atoms, respectively. Those values are smaller than 0.0808(16)  $\text{Å}^2$  of Ag atom at room temperature because the

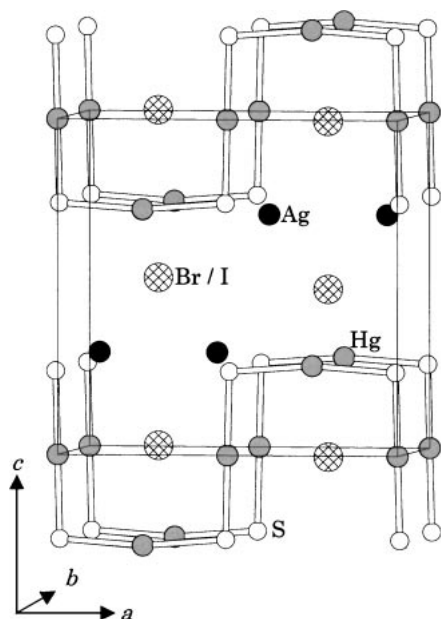


Fig. 11. The crystal structure of AgHgSBr and  $\beta$ -AgHgSI reported by Beck et al.<sup>4</sup>

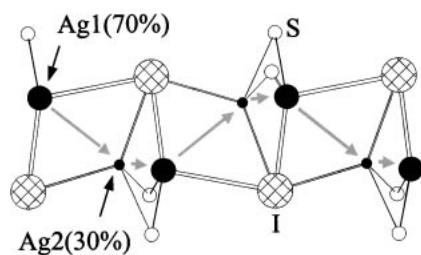


Fig. 12. The plausible ionic conduction path for  $\alpha$ -AgHgSI. Ag ion transfer between Ag1 sites can be achieved via adjacent Ag2 sites.

Ag site occupancies would be divided in two positions.

Figure 12 shows the plausible conduction path for  $\alpha$ -AgHgSI at 400 K. Since Ag2 site can be regarded as equivalent to Ag1 site, the Ag ion can easily transfer to the neighboring Ag1 sites through Ag2 site. The atomic distances between Ag1 and Ag2 sites at 400 K were 1.28(1) and 2.99(1) Å, though that of Ag site distance at room temperature was 4.09(2) Å. From the monotonous increasing between room temperature and 500 K for Ag conductivity, the electron density distribution at 400 K indicates the progressive dynamics up to the Ag<sup>+</sup> diffusion. Thus, the site occupancies of Ag1 and Ag2 sites will finally approach the equivalent occupancies at higher temperature. As Ag site occupancies are incomplete, at least at 400 K and above, the activation enthalpy shows only the Ag<sup>+</sup> ionic motion without producing the new defect sites for the Ag conduction.

**$\beta$ -AgHgSI and AgHgSBr:** For  $\beta$ -AgHgSI, the electron density maps of (010) plane are shown in Figs. 6 and 7. At 400 K, the overlap of electron densities between the neighboring Ag sites clearly shows the Ag<sup>+</sup> ion conduction path, as the electron densities on I, Hg, and S sites are localized.

Figures 8 and 9 illustrate the electron density maps for AgHgSBr along the (010) plane at room temperature and 500

K, respectively. As in the case of  $\beta$ -AgHgSI, the electron densities of Ag<sup>+</sup> ions at room temperature are quite different from the ones at 500 K: the overlap of electron densities between the neighboring Ag<sup>+</sup> ions are clearly visible at high temperature. On the other hand, the electron densities on Br, Hg, and S atoms are still confined to the small area.

These facts strongly indicate that Ag<sup>+</sup> ion transfer along the (100) direction in each compound.

**Comparisons for Conductivity.  $\alpha$ - and  $\beta$ -AgHgSI:** The Ag<sup>+</sup> ion conductivity of  $\alpha$ -AgHgSI is higher than that of  $\beta$ -AgHgSI. This result is explained by the defect formation in the crystal structure. For  $\alpha$ -AgHgSI, the new Ag2 site arises as an intermediate position between Ag1 sites at least at 400 K and above. On the other hand, the defect formation is necessary for  $\beta$ -AgHgSI to transfer Ag ions to neighboring sites, since all Ag sites are completely occupied. As for Ag atomic distances, 1.28(1) and 2.99(1) Å distances between Ag1 and Ag2 sites for  $\alpha$ -AgHgSI at 400 K are shorter than 3.68(2) and 4.29(1) Å distances between Ag atoms for  $\beta$ -AgHgSI. The Ag<sup>+</sup> ion in  $\alpha$ -AgHgSI is thus more mobile than that in  $\beta$ -AgHgSI. This distinction of the conduction mechanism reflects the magnitude of the activation enthalpy and the conductivity.

**$\beta$ -AgHgSI and AgHgSBr:** The Ag<sup>+</sup> ion conductivity of  $\beta$ -AgHgSI is higher than that of AgHgSBr. Since both compounds have the same structure, the difference of conductivity may be arise from the enlargement of the gap between halogens that determines the bottleneck for the Ag<sup>+</sup> ion dynamics.

## Conclusion

AgHgSX (X = Br, I) were successfully characterized in detail. AgHgSI has two modifications at room temperature. The crystal structure of the high temperature phase of AgHgSI was determined. Both compounds showed relatively higher electric conductivity due to Ag<sup>+</sup> ions. The ionic conduction mechanism was clearly described by the temperature dependence of the electron density distribution at Ag site.

## References

- 1 D. O. Religh, *J. Appl. Phys.*, **41**, 1876 (1970).
- 2 M. Guillo, B. Mercey, and A. Deschanvres, *Mater. Res. Bull.*, **14**, 947 (1979).
- 3 J. Beck and M. Rompel, *Z. Anorg. Allg. Chem.*, **629**, 421 (2003).
- 4 J. Beck, H. Keller, M. Romel, and L. Wimbirt, *Z. Anorg. Allg. Chem.*, **627**, 2289 (2001).
- 5 R. Blachnik and K. Lytze, *Thermochim. Acta*, **190**, 79 (1990).
- 6 C. Giacomazzo, D. Siliqi, B. Carrozzini, A. Guagliardi, and A. G. G. Moliterni, *J. Appl. Cryst.*, **32**, 339 (1999).
- 7 F. Izumi and T. Ikeda, *Mater. Sci. Forum*, **321–324**, 198 (2000).
- 8 F. Izumi, *Rigaku J.*, **17**, 34 (2000).
- 9 M. Moro'oka, H. Ohki, K. Yamada, and T. Okuda, *J. Solid State Chem.*, in press.
- 10 M. Moro'oka, H. Ohki, K. Yamada, and T. Okuda, *Bull. Chem. Soc. Jpn.*, **76**, 2111 (2003).
- 11 S. Chandra, "Superionic Solid, Principles and Applications," North-Holland Pub. Co., Amsterdam (1981), p. 225.